Influence of Seismic Pounding on Dynamic Response of Skewed Highway Bridges

Mohsen Amjadian
Master Engineer of Earthquake Engineering, Navid Bana Gharb Construction Company, Kermanshah, Iran.

Afshin Kalantari
Assistant Professor of Earthquake Engineering, Structural Engineering Research Centre (SERC), IIEES, Tehran, Iran.

SUMMARY
This paper aims to analytically reveal that how the rigid body motion of the deck in skewed highway bridges is affected by seismic pounding during a severe earthquake. For this purpose, a dynamic model with three degrees of freedom is developed to model the general dynamic features of skewed highway bridges. Then a parametric analysis is performed based on the variations of different parameters including the skewness angle (β), the width of expansion joint (gap), and the normalized stiffness eccentricity along the X axis (e_x/r). The numerical results indicate that seismic pounding has no noticeable effects on the transverse displacement and rotation of the deck in straight highway bridges, whereas these responses are considerably increased in skewed highway bridges. Furthermore, the amplification of transverse displacements in the acute corners of symmetric and asymmetric skewed highway bridges leading to the deck unseating, is more significant than that in the obtuse corners.

Keywords: skewed highway bridge; seismic pounding; parametric analysis.

1. INTRODUCTION

Today, due to the complexity of the interchanges shape and the lack of space in the urban areas, the skewed highway bridges are frequently employed to carry traffic in the urban transportation systems of metropolises. The irregular geometry of this type of bridge results in a unique seismic response during the ground excitation. The investigation of seismic behaviour of the skewed highway bridges in past earthquakes reveals that this type of bridge is more susceptible to the seismic damage in comparison with the straight highway bridges with regular geometry (Jennings et al, 1971). For instance, some damage in skewed highway bridges were reported by Kawashima et al (2010) in the recent severe earthquake of Chile on February 27, 2010. In this strong earthquake, Hospital and Copihue Overcrossings with skewness angles of about 60° and 45°, respectively, suffered a heavy damage because of in-plane rotation of the deck (Kawashima et al, 2010). Fig. 1.1 shows that the north-bound skewed bridge of Hospital Overcrossing experienced an irreparable damage due to clockwise rotation of the deck, while the south-bound straight bridge remained almost undamaged during this strong earthquake.

From a review of the technical literature (Maragakis, 1984, Maleki, 2001 and Tirasit and Kawashima, 2008), it can be concluded that the coupling of the translational motions of the deck and the seismic pounding are the most effective factors affecting the seismic behaviour of this type of bridge. Although, numerous studies have been carried out in this field, none of them have considered these factors simultaneously in modeling of the skewed highway bridges. For example, Kalantari and Amjadian (2010) investigated the effects of coupling of the translational motions and overlooked the influence of seismic pounding, whereas Dimitrakopoulos (2011) studied the effects of seismic pounding without considering the effects of coupling of the translational motions of the deck.

This paper using a simplified dynamic model, which considers the effects of coupling of the translational motions of the deck, investigates the influence of seismic pounding on the linear response of the superstructure in a sample skewed highway bridge. The model is based on the previous works of authors (Kalantari and Amjadian, 2010, 2011 and Amjadian, 2010).

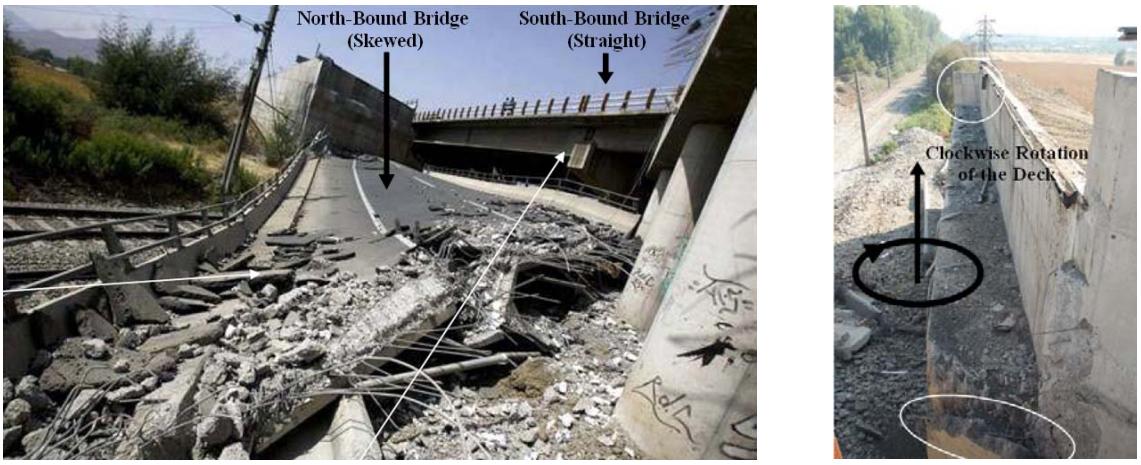

Figure 1.1. Seismic behaviour of the north-bound (skewed) and south-bound (straight) of Hospital Overcrossing during the Chile Earthquake on 27th Feb. 2010 (Picture Source: Kawashima et al, 2010)

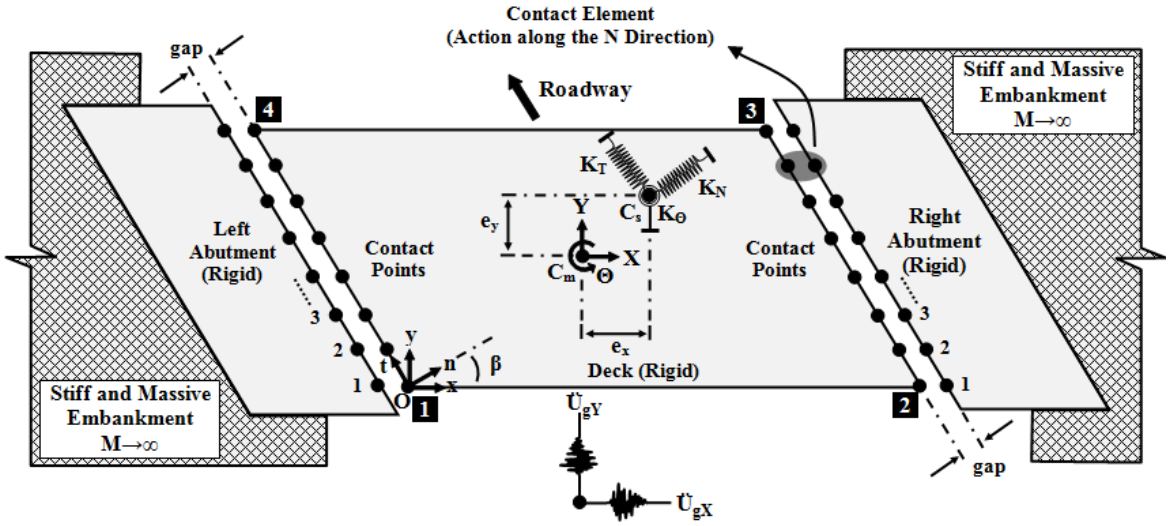

Figure 2.1. The 3DOF simplified model of a skewed highway bridge (β = skewness angle).

2. MATHEMATICAL MODELING OF THE PROBLEM

A simplified three degrees of freedom model is developed to model the problem, as shown in Fig. 2.1. To simplify the model, it is assumed that the deck remains rigid in its own plane and columns do not enter into the nonlinear part of their behaviour during the ground excitation. In the model, β is the skewness angle of the bridge, C_m (x_m,y_m) is the mass centre of the superstructure, and C_s (e_x,e_y) is the stiffness centre of the substructure. The governing equation of motion of the bridge model subjected to the bi-directional ground acceleration is as follows:

$$[M]\{\ddot{U}(t)\} + [C]\{\dot{U}(t)\} + [K]\{U(t)\} = -[M]\{\ddot{U}_g(t)\} - \{F_p(t)\} \tag{2.1}$$

Where [M], [C] and [K] are mass, damping and stiffness matrices of the model, respectively; $\{F_P(t)\}$ is the resultant vector of impact forces acting on the mass centre of the deck. The mass and stiffness matrices are defined as follows:

$$[M]=\begin{bmatrix} M & 0 & 0 \\ 0 & M & 0 \\ 0 & 0 & I \end{bmatrix}$$

$$[K]=\begin{bmatrix} K_{XX} & K_{XY} & -e_y K_{XX}+e_x K_{XY} \\ K_{XY} & K_{YY} & -e_y K_{XY}+e_x K_{YY} \\ -e_y K_{XX}+e_x K_{XY} & -e_y K_{XY}+e_x K_{YY} & e_y^2 K_{XX}-2e_x e_y K_{XY}+e_x^2 K_{YY}+K_\Theta \end{bmatrix} \tag{2.2}$$

With regard to Rayleigh method, the damping matrix is also defined as [C]=a[M]+b[K] (ξ =5%.). The resultant vector of impact forces denoted as $\{F_P(t)\}$ can be calculated by this formula:

$$\{F_p(t)\}=\begin{bmatrix} +\cos\beta & 0 & 0 \\ +\sin\beta & 0 & 0 \\ 0 & +\sin\beta & -\cos\beta \end{bmatrix}\times\left(\sum_{j=1}^{n_p}\begin{Bmatrix}1\\ x_{rj}\\ y_{rj}\end{Bmatrix}F_{PRj}(t)-\sum_{j=1}^{n_p}\begin{Bmatrix}1\\ x_{lj}\\ y_{lj}\end{Bmatrix}F_{PLj}(t)\right) \tag{2.3}$$

In which n_p is the number of contact points between the deck and the rigid abutments, vectors $\{1\ x_{rj}\ y_{rj}\}^T$ and $\{1\ x_{lj}\ y_{lj}\}^T$ are the locations of contact points with respect to the mass centre at the left and right abutments, respectively. $F_{PRj}(t)$ and $F_{PLj}(t)$ are the impact forces at contact points between the deck and the right and left abutments, respectively. These forces are calculated based on the contact element model employed to simulate the seismic pounding (Kalantari and Amjadian, 2011).

3. SEISMIC POUNDING SIMULATION

The nonlinear viscoelastic model is used to simulate the impact forces at the contact points (Jankowski 2004 and 2006). This model includes a nonlinear spring (k_p) in parallel with a nonlinear damper (c_p) which the spring acts based on the Hertz law of contact and the damper is applied to simulate the process of energy dissipation during contact. With regard to this model, $F_{PRj}(t)$ and $F_{PLj}(t)$ are calculated as follows (i=R $\rightarrow$ α = +1, i=L $\rightarrow$ α = -1):

$$F_{Pij}(t)=\begin{cases} k_p\delta_{ij}(t)^{3/2}+c_{pij}\dot{\delta}_{ij}(t) & \delta_{ij}(t)>0 \quad \dot{\delta}_{ij}(t)>0 \\ k_p\delta_{ij}(t)^{3/2} & \delta_{ij}(t)>0 \quad \dot{\delta}_{ij}(t)\le 0 \\ 0 & \delta_{ij}(t)\le 0 \end{cases}$$

$$c_{pij}=2\xi_p\sqrt{k_p M_{ej}\sqrt{\delta_{ij}(t)}} \tag{3.1}$$

$$\delta_{ij}(t)=\alpha[X(t)\cos\beta+Y(t)\sin\beta-\Theta(t)(-x_{ij}\sin\beta+y_{ij}\cos\beta)]-gap$$

$$\dot{\delta}_{ij}(t)=\alpha[\dot{X}(t)\cos\beta+\dot{Y}(t)\sin\beta-\dot{\Theta}(t)(-x_{ij}\sin\beta+y_{ij}\cos\beta)]$$

In which M_{ej} is the effective mass of the deck at each contact point and is defined as a proportion of the deck mass ($M_{ej}=\lambda_j M$).

4. NUMERICAL EXAMPLE

As a numerical example, the south eastern bridge of Foothill Boulevard Undercrossing (Jennings et al, 1971) is modeled with regard to the presented formulas. This skewed highway bridge is a four-span continuous reinforced concrete box girder bridge with a skewness angle of about 60˚ and $e_x/r\neq 0$, $e_y/r=0$. The plan-view of this bridge is shown in Fig. 4.1. In order to analyze the dynamic model, seven pairs of accelerograms as the input accelerations are selected from PEER strong ground motion database (web address: http://peer.berkeley-.edu/smcat/) and applied to the sample bridge along the

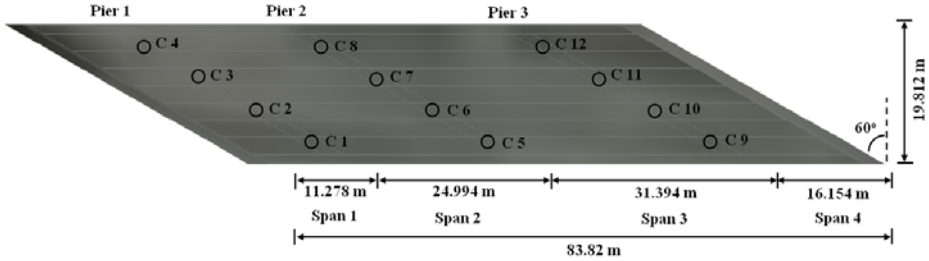

Figure 4.1. The plan-view of the south eastern bridge of Foothill Boulevard Undercrossing

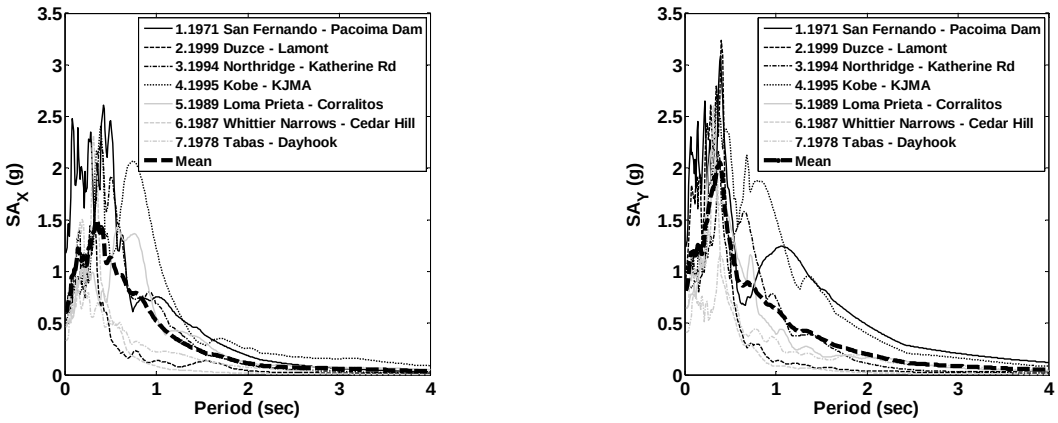

Figure 4.2. The absolute acceleration response spectrums of the seven pairs of accelerogram.

two orthogonal axes. To satisfy the stiff soil assumption, these accelerograms are taken out among sites with the stiff soil conditions. The absolute acceleration response spectrums of these ground motions along X and Y directions are shown in Fig. 4.2. To analyze the model, all of accelerograms are scaled to the mean spectral accelerations at the predominant period of the sample bridge (T_n=0.520 sec). The mean spectral accelerations along the X and Y directions at the predominant period are 1.111g and 1.168g, respectively. The matrix equation of motion (Eqn. 2.1) is implemented in SIMULINK that is software for modeling, simulating, and analyzing of dynamic systems. The matrix equation of motion is numerically solved using the 4th-order Runge-Kutta method denoted by ode4 in SIMULINK. The time-step is selected equal to 10^{-3} sec to smooth sudden changes of the system state due to the instantaneous transmission of a large stiffness to system during the contact period. This time-step is satisfactory for numerical integration of the equation because it sufficiently prevents the numerical errors and instability. It is clear that to simulate the colliding of the deck with abutments a specified number is required for contact points. It is assumed that the number of contact points is equal to 21 sufficient to accurately estimate the impact forces transmitted to the deck. The main parameters of the nonlinear viscoelastic contact model are the stiffness (k_p) and damping (ξ_p) parameters. The stiffness ratio (k_p) depends on the material properties and geometry of the colliding members and the damping ratio (ξ_p), which is a criterion for the energy dissipation during impact, depends on the restitution coefficient (e). Based on the experimental verification performed by Jankowski (2004) for concrete-to-concrete impact, the value of restitution coefficient is approximately equal to 0.65 and the value of damping ratio is calculated equal to 0.35. Furthermore, based on the results of this experiment, it is assumed that k_p is equal to 2.75×106 kN/m$^{1.5}$ at each contact point.

5. PARAMETRIC STUDY

To investigate the influence of seismic pounding on the linear responses of the sample bridge's deck, a parametric analysis is carried out under variations of different parameters. The parameters considered are: the width of expansion joints (gap), the skewness angle (β) and the normalized stiffness eccentricity along the X axis (e_x/r). The response quantities of interest are: the maximum transverse displacement of the deck corners, $(Y_{cpi})_P/(Y_{cpi})_{N.P}$, (i=1,2,3, and 4), the maximum rotation of the deck,

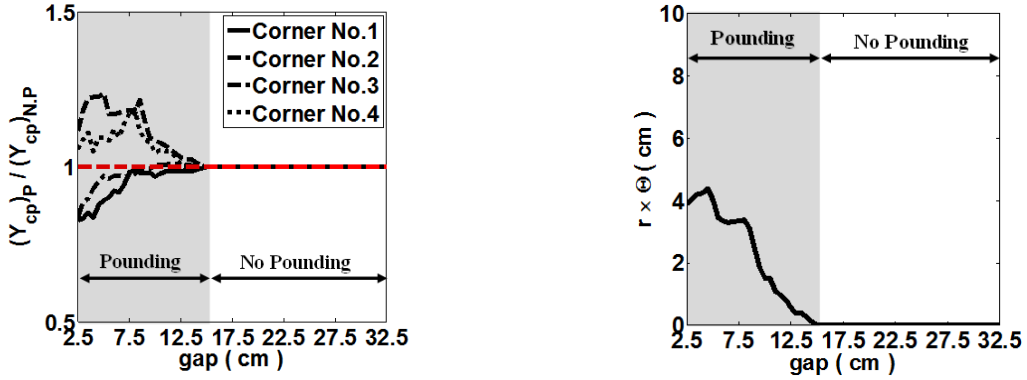

(a) (b)

Figure 5.1.1. Variation of the displacement of the deck versus different values of the width of expansion joints (β=60°, $e_x/r=e_y/r=0$), (a) ratio of the transverse displacements of corners, and (b) rotation of the deck.

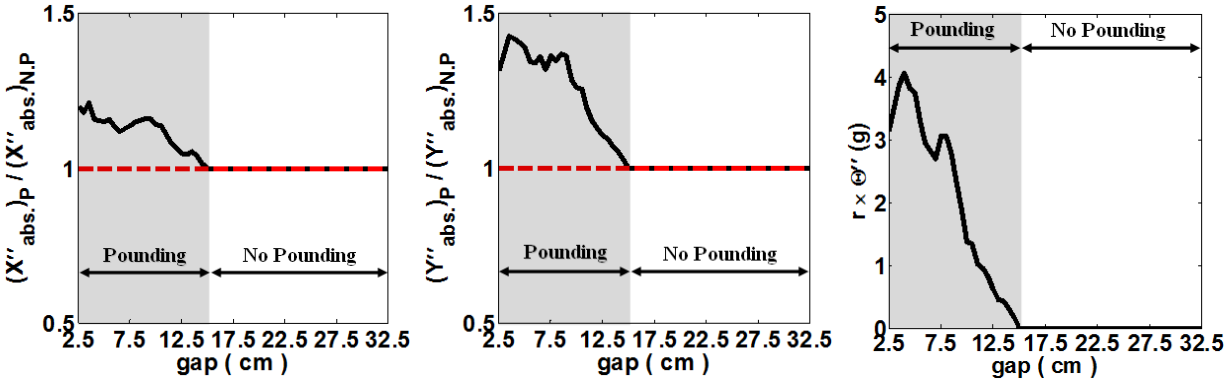

(a) (b) (c)

Figure 5.1.2. Variation of the acceleration of the deck versus different values of the width of expansion joints (β=60°, $e_x/r=e_y/r=0$), (a) longitudinal acceleration, (b) transverse acceleration, and (c) rotational acceleration.

$r\times\Theta$, the maximum absolute longitudinal acceleration of the deck, $(\ddot{X}_{abs})_P/(\ddot{X}_{abs})_{N.P}$, the maximum absolute transverse acceleration of the deck, $(\ddot{Y}_{abs})_P/(\ddot{Y}_{abs})_{N.P}$, and the maximum rotational acceleration of the deck, $r\times\ddot{\Theta}$. To more clearly study the effect of seismic pounding, the translational responses of the deck are stated as ratios in the case of pounding to the case of no pounding. Firstly, all of the responses under variations of mentioned parameters are calculated for all of the seven pairs of accelerograms and then averaged.

5.1. Influence of the width of expansion joints (gap).

The size of gap is varied from 2.5cm up to 32.5cm and it is assumed that the skewed bridge is symmetric ($e_x/r=e_y/r=0$) with the skewness angle (β) equal to 60°. The result presented in Fig. 5.1.1.a is the ratio of $(Y_{cp})_P/(Y_{cp})_{N.P}$ calculated for the corners of 1, 2, 3, and 4. This figure shows that the collision of the deck with abutments noticeably influences the transverse displacement of corners. As can be seen the seismic pounding increases the transverse displacements of the acute corners (i.e. corners of 2 and 4) and decreases the transverse displacements of the obtuse corners (i.e. corners of 1 and 3). It is also observed that major variations occur in the small sizes of gap, whereas these variations are reduced by increasing the width of expansion joints. The variations of the deck rotation are also shown in Fig. 5.1.1.b. The results show that the seismic pounding amplifies the rotation of the deck in small values of the width of expansion joints; however, this response is reduced by increasing the size of gap. This point should be considered that the torsional moments of columns have a direct relationship with the rotation of the deck.

Fig. 5.1.2.a and 5.1.2.b present the ratio of $(\ddot{X}_{abs.})_P/(\ddot{X}_{abs.})_{N.P}$ and $(\ddot{Y}_{abs.})_P/(\ddot{Y}_{abs.})_{N.P}$, respectively. As can be observed the seismic pounding significantly increases the transverse acceleration of the deck by more than 25%, while its effect on the longitudinal acceleration of the deck is not so noticeable (the

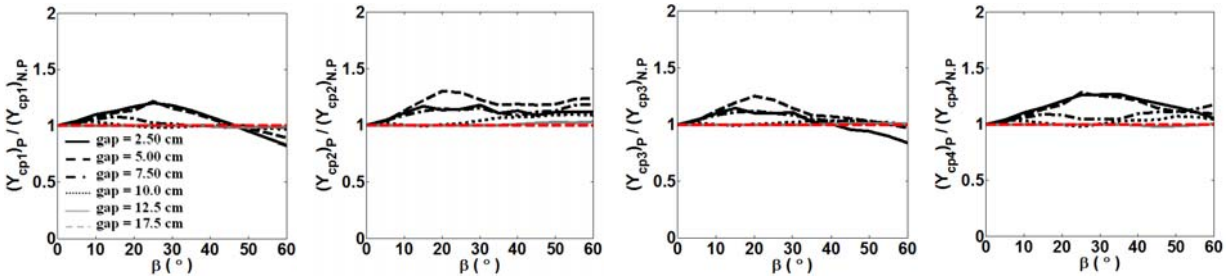

(a) (b) (c) (d)

Figure 5.2.1. Variation of the transverse displacement of the deck corners versus different values of the skewness angle ($e_x/r=e_y/r=0$), (a) corner No.1, (b) corner No.2, (c) corner No.3 and (d) corner No.4.

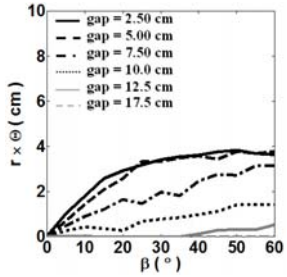

Figure 5.2.2. Variation of the rotation of the deck versus different values of the skewness angle ($e_x/r=e_y/r=0$).

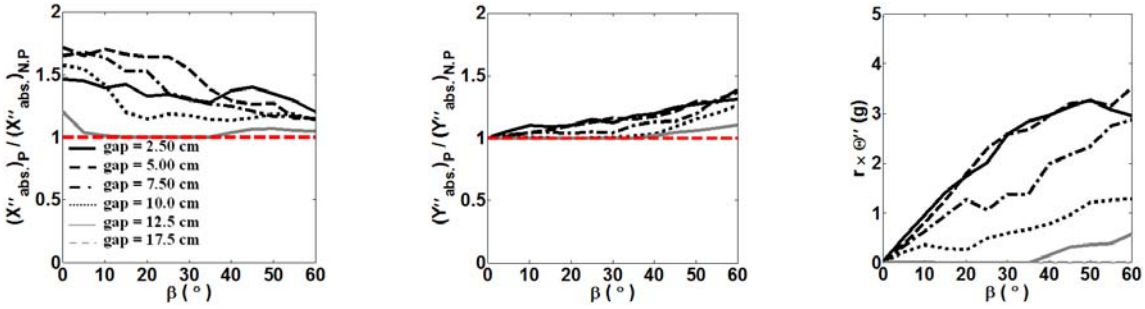

(a) (b) (c)

Figure 5.2.3. Variation of the acceleration of the deck versus different values of the skewness angle ($e_x/r=e_y/r=0$), (a) longitudinal acceleration, (b) transverse acceleration, and (c) rotational acceleration.

amplification is less than 25%). Presented in Fig. 5.1.2.c indicates that the seismic pounding has also significant effects on the rotational acceleration of the deck. In general, it can be concluded that by reduction of the width of expansion joints which raises the possibility of seismic pounding, the transmitted impact forces amplify the rotational acceleration of the deck.

5.2. Influence of the skewness angle (β).

The value of β is varied from 0° up to 60°. It is assumed that the skewed bridge is symmetric ($e_x/r=e_y/r=0$) and the width of expansion joints is equal to 2.5, 5.0, 7.5, 10.0, 12.5 and 17.5 cm. Presented in Fig. 5.2.1 is the ratio of $(Y_{cp})_P/(Y_{cp})_{N.P}$ calculated for the corners of 1, 2, 3, and 4. As may be seen in this figure, the collision of the deck with abutments increases the transverse displacements of the acute corners (i.e. corners 2 and 4) in all of skewness angles. The considerable increase in this response is observed in the moderate skewness angle (15° up to 35°) and the small sizes of gap (2.5 and 5.0 cm). Similarly, the significant increase in the transverse displacements of obtuse corners (i.e. corners 1 and 3) is observed in the moderate skewness angle and the small sizes of gap. However, the collision decreases this response in the large skewness angles (more than 50°) and the small sizes of gap. The curves presented in Fig. 5.2.2 show the variations of rotation of the deck. It is observed that the rotation of the deck is considerably amplified by increasing the skewness angle and decreasing of the width of expansion joints. Hence, in the symmetric skewed highway bridges with large skewness angles and the small sizes of gap, it can be expected that the seismic pounding amplifies the seismic

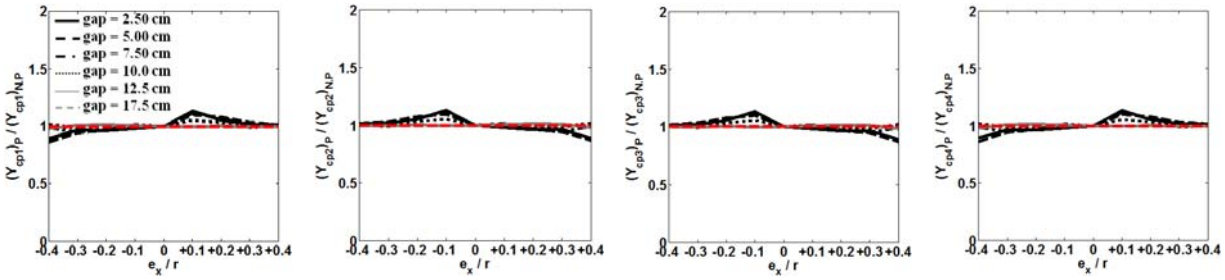

(a) (b) (c) (d)

Figure 5.3.1. Variation of the transverse displacement of the deck corners versus different values of the normalized stiffness eccentricity (β=0°), (a) corner No.1, (b) corner No.2, (c) corner No.3 and (d) corner No.4.

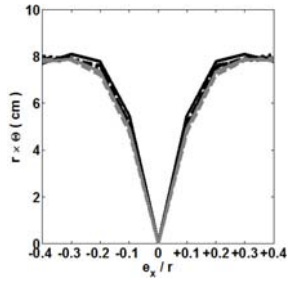

Figure 5.3.2. Variation of the rotation of the deck versus different values of the normalized stiffness eccentricity (β=0°).

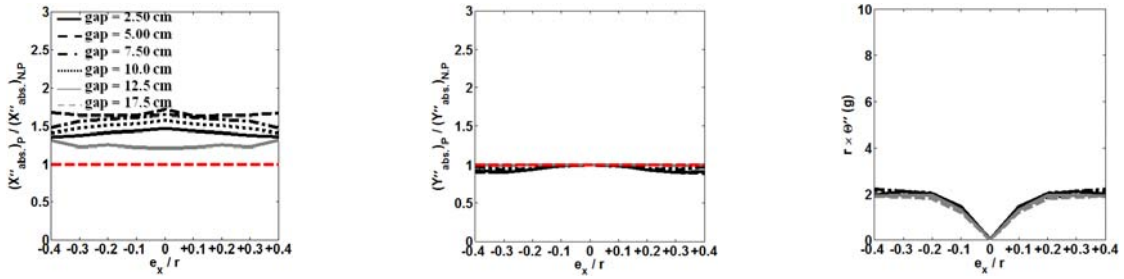

(a) (b) (c)

Figure 5.3.3. Variation of the acceleration of the deck versus different values of the normalized stiffness eccentricity (β=0°), (a) longitudinal acceleration, (b) transverse acceleration, and (c) rotational acceleration.

demand of torsional moments of columns ($T_\theta=k_\theta\Theta$) from zero to a significant value.

Fig. 5.2.3.a and 5.2.3.b show the ratio of $(\ddot{X}_{abs})_P/(\ddot{X}_{abs})_{N.P}$ and $(\ddot{Y}_{abs})_P/(\ddot{Y}_{abs})_{N.P}$ for different skewness angles, respectively. As may be seen increasing β decreases the longitudinal acceleration of the deck and increases the transverse acceleration of the deck. However, both of two ratios are increased over the range of β by decreasing of the gap size considered. Fig. 5.2.3.c indicates the effects of variations of skewness angle on increasing rotational acceleration of the deck. As can be seen in this figure, the rotational acceleration of the deck is significantly amplified by increasing the skewness angle and reduction of the width of expansion joints.

5.3. Influence of the normalized stiffness eccentricity along the X axis (e_x/r).

The normalized stiffness eccentricity of the sample bridge is varied along the X axis. For this purpose, the lengths of the second and third spans of the sample bridge are varied, but the lengths of the first and fourth spans remain equal to 11.278 m. Therefore, e_x/r becomes equal to 0.00, ±0.104, ±0.207, ±0.309, and ±0.407. In this part of study, two skewness angles of β=0° (straight) and β=60° (skewed) are considered, and it is also assumed that the width of expansion joints is varied as 2.5, 5.0, 7.5, 10.0, 12.5 and 17.5 cm. Fig. 5.3.1 to 5.3.3 and Fig. 5.3.4 to 5.3.6 present the seismic responses of the straight and skewed bridges, respectively.

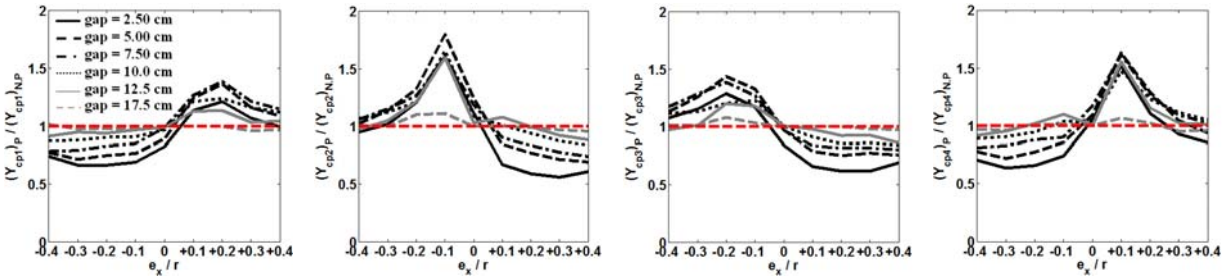

Figure 5.3.4. Variation of the transverse displacement of the deck corners versus different values of the normalized stiffness eccentricity (β=60°), (a) corner No.1, (b) corner No.2, (c) corner No.3 and (d) corner No.4.

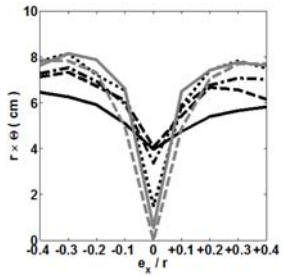

Figure 5.3.5. Variation of the rotation of the deck versus different values of the normalized stiffness eccentricity (β=60°).

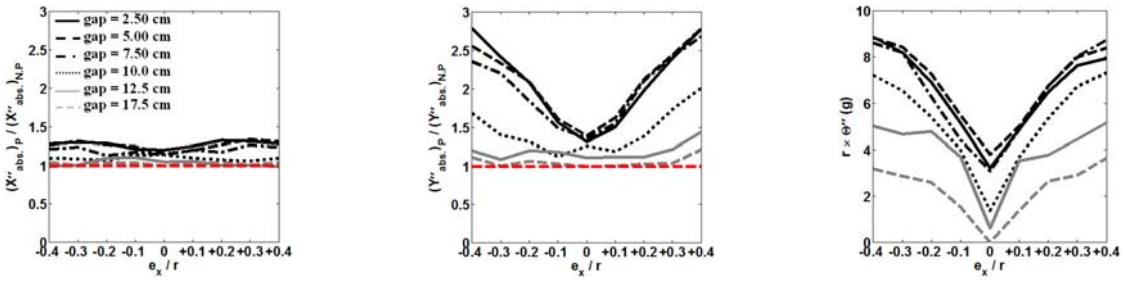

Figure 5.3.6. Variation of the acceleration of the deck versus different values of the normalized stiffness eccentricity (β=60°), (a) longitudinal acceleration, (b) transverse acceleration, and (c) rotational acceleration.

The result presented in Fig. 5.3.1 is the ratio of $(Y_{cp})_P/(Y_{cp})_{N.P}$ calculated for the corners of 1, 2, 3, and 4 in the straight bridge. This figure shows that the variations of e_x/r, in contrast to what is expected, have no noticeable effects on the transverse displacements of corners. Nevertheless, for e_x/r=-0.4 representing the farthest distance of corners of 2 and 3 from the stiffness centre, the ratios of $(Y_{cp1})_P/(Y_{cp1})_{N.P}$ and $(Y_{cp4})_P/(Y_{cp4})_{N.P}$ are reduced, while the ratios of $(Y_{cp2})_P/(Y_{cp2})_{N.P}$ and $(Y_{cp3})_P/(Y_{cp3})_{N.P}$ for all sizes of the gap remain at a constant value which is equal to one. After transmission of the stiffness centre toward the right side, the transverse displacements of all four corners are increased. When e_x/r becomes equal to -0.1, $(Y_{cp2})_P/(Y_{cp2})_{N.P}$ and $(Y_{cp3})_P/(Y_{cp3})_{N.P}$ reach their maximum value equal to 1.13 which emerge in the small sizes of gap. On the other hand, $(Y_{cp1})_P/(Y_{cp1})_{N.P}$ and $(Y_{cp4})_P/(Y_{cp4})_{N.P}$ approximately become equal to one. After passing the stiffness centre through the mass centre, the corners inversely and approximately follow the trend mentioned above. Fig. 5.3.2 indicates the rotation of the deck. The figure indicates that the rotation of the deck is symmetrically amplified by increasing the absolute value of e_x/r. Moreover, it is seen that variations of the gap size has no evident effects on the rotation of the deck, while the eccentricity of the stiffness centre is more effective on this response. The variations of the ratios of $(\ddot{X}_{abs})_P/(\ddot{X}_{abs})_{N.P}$ and $(\ddot{Y}_{abs})_P/(\ddot{Y}_{abs})_{N.P}$ in the straight bridge versus the variations of e_x/r are shown in Fig. 5.3.3.a and 5.3.3.b. Based on the fact that impact forces act along the longitudinal axis of the deck in straight bridges, so it is seen that the ratio of $(\ddot{X}_{abs})_P/(\ddot{X}_{abs})_{N.P}$ for different values of e_x/r is increased by the seismic pounding. However, this increasing is somewhat different for different values of the gap size. As this figure indicates the ratio of $(\ddot{X}_{abs})_P/(\ddot{X}_{abs})_{N.P}$ is reduced by increasing the value of the gap size, while the effect

of variations of e_x/r on this response for a specified value of the gap size is almost constant. It is also observed that the variations of e_x/r have no noticeable effects on the transverse acceleration of the deck, and so this response for different values of e_x/r and the gap size almost remains constant. The rotational acceleration of the straight bridge versus variations of e_x/r is presented in Fig. 5.3.3.c. It is seen that increasing the absolute value of e_x/r amplifies the response. Moreover, it is evident that the variations of the gap size do not affect this response.

The seismic response of the skewed bridge (β=60) is evaluated here. Presented in Fig. 5.3.4 is the ratio of $(Y_{cp})_P/(Y_{cp})_{N.P}$ calculated for the corners of 1, 2, 3, and 4 in the skewed bridge. This figure implies that the variations of e_x/r have noticeable effects on the transverse displacements of corners. As it is expected, this influence is more observable in the acute corners of the skewed bridge's deck (i.e. corners 2 and 4). Fig. 5.3.5 shows the rotation of the deck. As may be seen in this figure, the variations of e_x/r cause a noticeable amplification in the rotation of the deck of the skewed bridge. This response is varied for different values of the gap size. It is observed that the rotation of the deck is increased by increasing the absolute value of e_x/r and enlarging of the gap size. In the case of the symmetric skewed bridge, the rotation of the deck is amplified by decreasing the sizes of gap; however, for the high asymmetric skewed bridges (i.e. $|e_x/r|>0.2$), the rotation of the deck is reduced by decreasing the sizes of gap. The variations of the ratios of $(\ddot{X}_{abs})_P/(\ddot{X}_{abs})_{N.P}$ and $(\ddot{Y}_{abs})_P/(\ddot{Y}_{abs})_{N.P}$ in the skewed bridge versus the variations of e_x/r are shown in Fig. 5.3.6.a and 5.3.6.b. It can be seen that, although collision of the deck with abutments increases both longitudinal and transverse acceleration, the effects of variations of e_x/r on the ratio of $(\ddot{Y}_{abs})_P/(\ddot{Y}_{abs})_{N.P}$ are more tangible than the ratio of $(\ddot{X}_{abs})_P/(\ddot{X}_{abs})_{N.P}$. For different values of the gap size, the transverse acceleration of the skewed bridge is amplified by increasing the absolute value of e_x/r; however, this amplification is more obvious in small sizes of gap. Fig. 5.3.6.c shows variations of the rotational acceleration of the skewed bridge's deck versus variations of e_x/r. This figure indicates that increasing the absolute value of e_x/r amplifies the rotational acceleration, and moreover, it shows that this response has much larger values in the small sizes of gap.

6. CONCLUSION

This paper presents a 3DOF dynamic model to analyze the unique seismic response of skewed highway bridges during the ground excitation. The collision of the deck with abutments is modeled by putting some contact points between the deck and abutments. The nonlinear viscoelastic contact model is employed to simulate the impact forces generated at contact points. Then, a parametric study is carried out on the numerical example to investigate the influence of seismic pounding on the linear responses of the deck. The applicable results obtained from the parametric study can be briefly stated as follows:

1- Unseating of the deck in abutments due to failure of side walls is very probable during a strong earthquake. Hence, investigation of the transverse displacements of corners of the deck amplified by the seismic pounding is essential in highway bridges. In general, seismic pounding has no noticeable effects on the transverse displacements of corners of the deck in the symmetric straight highway bridges. In the asymmetric straight highway bridges; however, this response depending on the distance of corners from the stiffness centre may be increased or decreased. On the other hand, in the symmetric skewed highway bridges with moderate skewness angles (β=15°~35°) and the small sizes of gap (gap=2.5~5.0cm), the seismic pounding leads to a considerable increase in the transverse displacements of all of the four corners. For large values of the skewness angle ($\beta\geq$50°), the transverse displacements of the acute corners is larger than those in the obtuse corners. This trend is also more obvious for the small sizes of gap (gap=2.5~5.0cm).

2- The seismic demand of torsional moments of columns has a direct relationship with the rotation of the deck. Therefore, investigation of the rotation of the deck amplified by the seismic pounding is important in seismic analysis of highway bridges. Although, asymmetry of the substructure considerably increases the rotation of deck in the straight highway bridges,

the seismic pounding has no evident effects on the rotation of the deck of this type of bridges for both of the symmetric and asymmetric cases. The rotation of the deck induced by seismic pounding is significantly increased by increasing the skewness angle and reduction of the gap size in the symmetric skewed highway bridges. In the skewed highway bridges with much larger skewness angles, the rotation of the deck is increased by increasing the asymmetry of the substructure. The effect of asymmetry on this response is more than the effect of seismic pounding in large sizes of gap.

3- The seismic pounding has no evident effects on the transverse and rotational acceleration of the deck in the symmetric and asymmetric straight highway bridges; however, it increases the longitudinal acceleration. The transverse and rotational accelerations are increased by increasing the skewness angle and reduction of the gap size, whereas this reduction is much less in the small sizes of gap. The asymmetry of the substructure has no noticeable influences on the longitudinal acceleration of the skewed highway bridges with large skewness angle. On the other hand, its effect on increasing the transverse and rotational accelerations is considerable and the maximum amplification is observed in small sizes of gap.

REFERENCES

Jennings P.C., Housner G.W., Hudson D.E., Trifunac M.D., Frazier G.A., Wood J.H., Scott R.F., Iwan W.D., Brady A.G. (1971). Engineering features of the San Fernando earthquake of February 9, 1971. Report No. EERL 71-02, Pasadena, California.

Kawashima K., Unjoh S., Hoshikuma J. and Kosa K. (2010). Damage of Bridges due to 2010 Chile Earthquake. *4th WFEO-JFES-JSCE Joint International Symposium on Disaster Risk Management, Sapporo, Japan*. **7-21**.

Maragakis E. (1984). A model for the rigid body motions of skew bridges. PhD Thesis, California Institute of Technology, Pasadena, CA.

Maleki S. (2001). Free vibration of skewed bridges. *Journal of Vibration and Control*. **7:7**, 935-952.

Tirasit P. and Kawashima K. (2008). Effect of Nonlinear Seismic Torsion on the Performance of Skewed Bridge Piers. *Journal of Earthquake Engineering*. **12**, 980-998.

Kalantari A. and Amjadian M. (2010). An approximate method for dynamic analysis of skewed highway bridges with continuous rigid deck. *Journal of Engineering Structures.* **32**, 2850-2860.

Dimitrakopoulos E.G. (2011). Seismic response analysis of skew bridges with pounding deck-abutment joints. *Journal of Engineering Structures*.

Kalantari A. and Amjadian M. (2011). Investigation of the seismic pounding effect on torsional response of highway bridges. *6th International Conference of Seismology and Earthquake Engineering, Tehran, Iran, 16-18 May*. Code:10123.

Amjadian M. (2010). Seismic behavior control of a skewed highway bridge using passive (seismic isolation) and semi-active methods (In Farsi). M.Sc. Thesis, Structural Engineering Research Centre, International Institute of Earthquake Engineering and Seismology, Tehran, Iran.

Jankowski R. (2004). Non-linear viscoelastic modeling of earthquake-induced structural pounding. *Journal of Earthquake Engineering and Structural Dynamic*. **34**, 595-611.

Jankowski R. (2006). Analytical expression between the impact damping ratio and the coefficient of restitution in the non-linear viscoelastic model of structural pounding. *Journal of Earthquake Engineering and Structural Dynamic*. **35**, 517-524.